# Dynamics of Coupled Chaotic Bonhoeffer – van der Pol Oscillators

I M. KYPRIANIDIS, V. PAPACHRISTOU, I. N. STOUBOULOS
Physics Department
Aristotle University of Thessaloniki
Thessaloniki 54124
GREECE
imkypr@auth.gr, vpapachr@el.teithe.gr, stouboulos@physics.auth.gr

CH. K. VOLOS
Department of Mathematics and Engineering Studies
University of Military Education - Hellenic Army Academy
Athens, GR-16673
GREECE
chvolos@gmail.com

*Abstract:* - In the present paper, we have studied the dynamics of coupled chaotic Bonhoeffer – van der Pol (BvP) electrical oscillators. In the case of series connection and bidirectional coupling via linear resistor, as the coupling strength varies, the chaotic states are driven to periodic states. In the case of ring-type connection, synchronization is observed in the case that the voltage driven BvP oscillator have different circuit parameters than the two identical current-driven BvP oscillators. The Bonhoeffer – van der Pol (BvP) electrical nonlinear oscillators simulate neuron cells and in this case the linear coupling resistors act as electric synapses. These synapses varying their resistance control the dynamics of the neuron cells, from chaotic to periodic states.

*Key-Words*: - Bonhoeffer – van der Pol, nonlinear electrical oscillators, chaos control, chaotic synchronization, bidirectional coupling, neuron cells, electric synapse, electronic simulator, antimonotonicity.

## 1 Introduction

As the understanding of chaotic behavior has been deepend, a significant interest in the problem of controlling chaotic dynamics of nonlinear systems has been observed [1-5].

After the pioneering work of Ott, Grebogi and Yorke [6], several algorithms have been developed to achieve control of chaotic behavior in nonlinear dynamical systems. Patidar et al. [7], have shown, that in the case of two bidirectionally coupled nonlinear oscillators of the same kind, one periodic and one chaotic, chaotic behavior is converted into the desired periodic behavior, as the coupling factor is varied, while Kyprianidis et al. [8] have shown that chaotic behavior is converted into the desired periodic behavior, in both coupled schemes, unidirectional and bidirectional.

The notion of chaotic synchronization was introduced by Pecora and Carroll [9] in 1990. A wide range of research activity, in a variety of complex physical, chemical and biological systems has been stimulated, ever since [10-13]. In particular, the topic of synchronization of coupled chaotic electronic circuits has been studied intensively [14-15].

Chaos control and synchronization have important potential applications [16-18] in several scientific areas including biology [19], medicine [20], electric circuits [21-27], laser technology [28-30], secure communication [31-34], and neuroscience [35-37] to name but a few.

The system of two FitzHugh-Nagumo cells coupled with gap junctions is the simplest possible system simulating two coupled neuron cells via an electric synapse [38]. As introduced by Fitzhugh [39], the BvP model for a spiking neuron is a two dimensional reduction of the Hodgkin – Huxley equations [40]. A qualitative description of the single neuron activity is given, according to FitzHugh, by the system of coupled nonlinear differential equations:

$$\begin{cases} \dot{x} = \gamma\left( x - \frac{1}{3}x^3 + y + z \right) \\ \dot{y} = -\frac{1}{\gamma}\left( x - \alpha + \beta y \right) \end{cases} \tag{1}$$

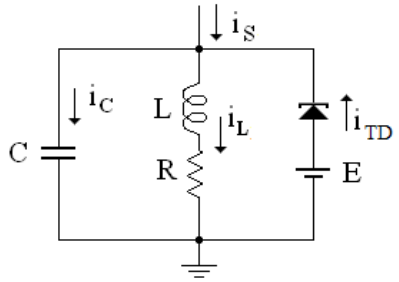


Fig.1. The electronic simulator of the BvP model proposed by Nagumo et al. [41].

The variable x describes the potential difference across the neural membrane and y can be considered as a combination of the different ion channel conductivities, present in the Hodgkin-Huxley model. The control parameter z of the BvP system describes the intensity of the stimulating current. Nagumo et al. [41] proposed an electronic simulator of the BvP model of FitzHugh using a tunnel diode as the nonlinear element (Fig.1).

The BvP model of nonlinear differential equations (1) can be simulated by a different nonlinear electric circuit (Fig.2), using a nonlinear resistor with a smooth cubic i-v characteristic.

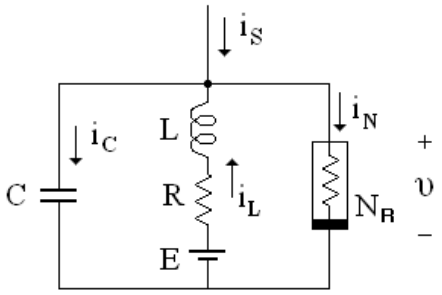


Fig.2. The electronic simulator of the BvP model of FitzHugh, proposed in the present paper.

## 2 Analysis of the New BvP Model

The smooth cubic i-v characteristic of the nonlinear resistor of the circuit of Fig.2 is given by the following equation:

$$i_N = g(\upsilon) = -\frac{1}{\rho}\left(\upsilon - \frac{1}{3}\frac{\upsilon^3}{V_0^2}\right) \tag{2}$$

where $\rho$ and $V_0$ are normalization parameters. From Kirchhoff's laws:

$$i_C - i_L + i_N = i_S \tag{3}$$

and

$$\upsilon = E - Ri_L - L\frac{di_L}{dt} \tag{4}$$

or

$$\frac{d\upsilon}{dt} = \frac{1}{C}\left\{\frac{1}{\rho}\left(\upsilon - \frac{1}{3}\frac{\upsilon^3}{V_0^2}\right) + i_L + i_S\right\} \tag{5}$$

and

$$\frac{di_L}{dt} = \frac{1}{L}\left(-\upsilon - Ri_L + E\right) \tag{6}$$

By introducing new, normalized variables, $\tau = \frac{t}{\sqrt{LC}}$, $x = \frac{\upsilon}{V_0}$, $y = \frac{\rho i_L}{V_0}$, and $z = \frac{\rho i_S}{V_0}$, equations (5) and (6) are reduced to equations (7) and (8).

$$\frac{dx}{d\tau} = \gamma\left(x - \frac{1}{3}x^3 + y + z\right) \tag{7}$$

$$\frac{dy}{d\tau} = \frac{1}{\gamma}\left(-x - \beta y + \alpha\right) \tag{8}$$

where

$$\alpha = \frac{E}{V_0}\ ,\ \beta = \frac{R}{\rho}\ \text{ and }\ \gamma = \frac{1}{\rho}\sqrt{\frac{L}{C}} \tag{9}$$

The nonlinear differential equations (7) and (8) are the FitzHugh equations (1).

### 2.1 The BvP model proposed by Rajasekar and Lakshmanan

Rajasekar and Lakshmanan proposed a slightly different form of BvP oscillator [42,43] given by the following state equations:

$$\begin{cases} \dfrac{dx}{d\tau} = x - \dfrac{1}{3}x^3 - y + z \\ \dfrac{dy}{d\tau} = c\left(x + a - by\right) \end{cases} \tag{10}$$

The study of Eqs.(10) revealed the existence of chaotic behavior, following the period doubling route to chaos, and devil's staircases. The nonlinear differential equations (10) can be also simulated by a nonlinear electric circuit, using a nonlinear resistor

with a smooth cubic i-v characteristic. The nonlinear electric circuit is shown in Fig.3. The smooth cubic i-v characteristic of the nonlinear resistor of the circuit of Fig.3 is given by the same equation, as before,

$$i_N = g(\upsilon) = -\frac{1}{\rho}\left(\upsilon - \frac{1}{3}\frac{\upsilon^3}{V_0^2}\right) \qquad (11)$$

where ρ and $V_0$ are normalization parameters. From Kirchhoff's laws:

$$i_C + i_L + i_N = i_S \qquad (12)$$

and

$$\upsilon = -E + Ri_L + L\frac{di_L}{dt} \qquad (13)$$

By introducing new, normalized variables $\tau = \frac{t}{\rho C}$, $x = \frac{\upsilon}{V_0}$, $y = \frac{\rho i_L}{V_0}$, and $z = \frac{\rho i_S}{V_0}$, equations (12) and (13) are reduced to equations (10), where,

$$a = \frac{E}{V_0} \ , \ b = \frac{R}{\rho} \ \text{and} \ c = \frac{\rho^2 C}{L} \qquad (14)$$

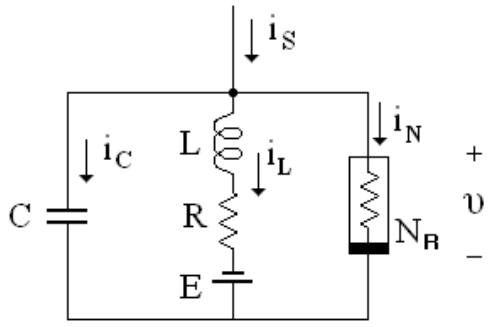


Fig.3. The nonlinear electric circuit simulating Eqs.(10).

The topology of the circuits of Fig.2 and Fig.3 is exactly the same, proving the equivalence of equations (1) and (10).

## 3 BvP Electrical Oscillator Driven by a Voltage Source

In the circuits of Figures 2 and 3, the driving source is a current source. But in most cases, circuits are driven by voltage sources. In this section, we will study the circuit of Fig.3 driven by a voltage source, as it is shown in Fig.4.

The smooth cubic i-v characteristic of the nonlinear resistor of the circuit of Fig.4 remains the same as before,

$$i_N = g(\upsilon) = -\frac{1}{\rho}\left(\upsilon - \frac{1}{3}\frac{\upsilon^3}{V_0^2}\right) \qquad (15)$$

and applying Kirhhoff's laws we have:

$$i_C + i_L + i_N = i_S \qquad (16)$$

where

$$i_S = \frac{\upsilon_S - \upsilon}{R_S} \qquad (17)$$

and

$$\upsilon = -E + Ri_L + L\frac{di_L}{dt} \qquad (18)$$

The normalized time, $\tau = \frac{t}{\rho C}$ and the normalized variables are:

$$x = \frac{\upsilon}{V_0} \ , \ y = \frac{\rho i_L}{V_0} \ , \ u = \frac{\rho \upsilon_S}{R_S V_0} \qquad (19)$$

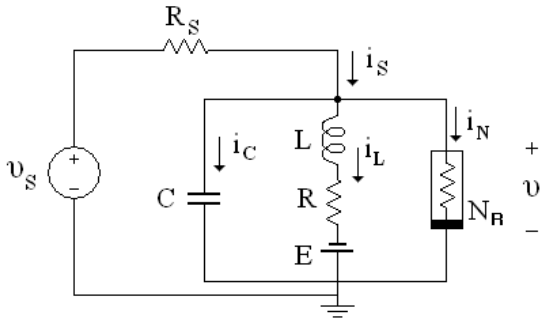


Fig.4. The equivalent circuit of BvP oscillator's state equations by Rajasekar and Lakshmanan driven by a voltage source.

Then the normalized state equations are the following.

$$\begin{cases} \dfrac{dx}{d\tau} = x(1-\varepsilon) - \dfrac{1}{3}x^3 - y + u \\ \dfrac{dy}{d\tau} = c(x + a - by) \end{cases} \quad (20)$$

where

$$a = \frac{E}{V_0},\ b = \frac{R}{\rho},\ c = \frac{\rho^2 C}{L} \text{ and } \varepsilon = \frac{\rho}{R_S} \quad (21)$$

In the general case, the driving voltage source has the following form:

$$\upsilon_S = B_S + B_0 \cos 2\pi f t \quad (22)$$

including a DC plus a sinusoidal term of frequency f, so:

$$u = U_S + U_0 \cos 2\pi f_N \tau \quad (23)$$

where the normalized frequency $f_N$ will be $f_N = \rho C f$.

As we can observe, this circuit driven by a voltage source has one additional circuit parameter, ε, in relation to the current driven circuits of Figures 2 and 3, which enriches the complexity of its dynamics.

### 3.1 Dynamics of the circuit – Bifurcation diagrams

We have studied the dynamics of the circuit keeping constant the following parameters: a = 0.7, b = 0.8, c = 0.1, $f_N$ = 0.160 and $U_S$ = 0.0. The birurcation diagrams, y vs. $U_0$, for different values of factor ε, are shown in the following figures 5-8 and antimonotonicity, forward and reverse period doubling sequences, is observed [44-47].

## 4 The Coupled System

By coupling the circuits of Figures 3 and 4 via a linear resistor, we get the system of Fig.9. The two sub-circuits have identical circuit elements, L, R, C, E and $N_R$ .

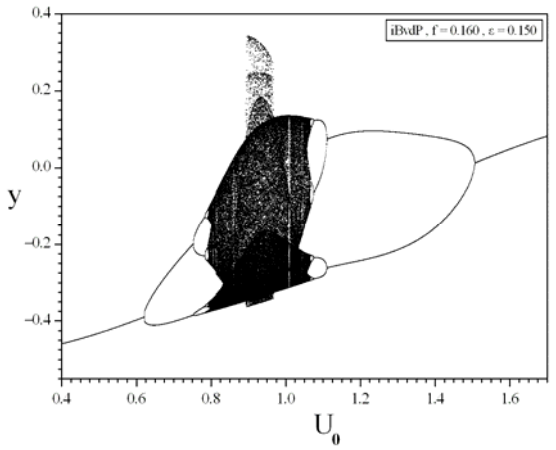


Fig.5. Bifurcation diagram, y vs. $U_0$, for ε = 0.150.

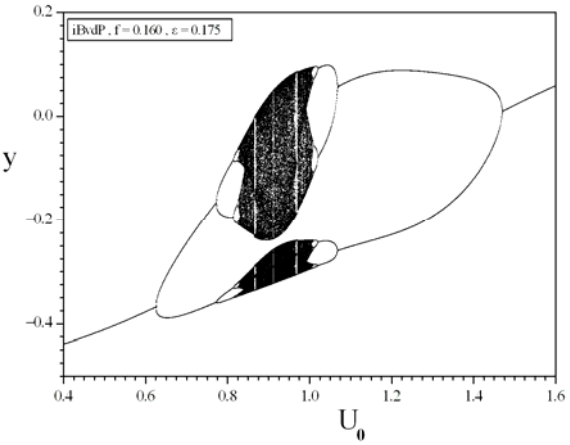


Fig.6. Bifurcation diagram, y vs. $U_0$, for ε = 0.175.

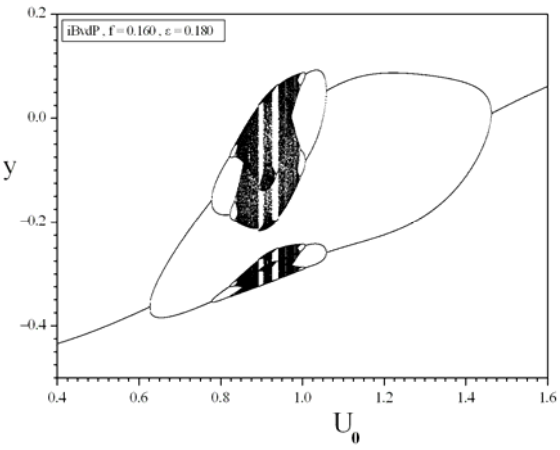


Fig.7. Bifurcation diagram, y vs. $U_0$, for ε = 0.180.

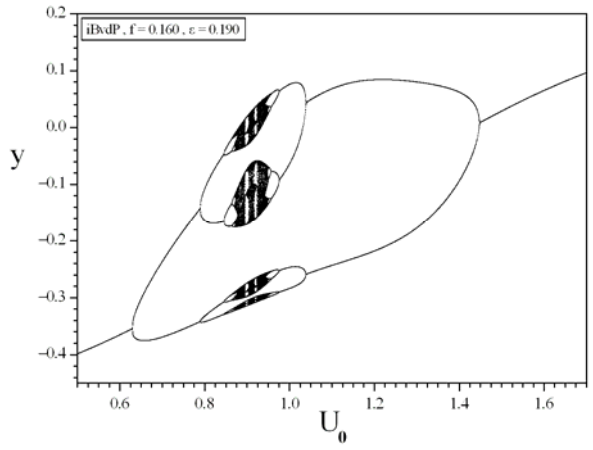


Fig.8. Bifurcation diagram, y vs. $U_0$, for ε = 0.190.

The normalized state equations of the system are:

$$\begin{cases} \dfrac{dx_1}{d\tau} = x_1(1-\varepsilon) - \dfrac{1}{3}x_1^3 - y_1 - \xi(x_1 - x_2) + u_S \\ \dfrac{dy_1}{d\tau} = c(x_1 + a - by_1) \\ \dfrac{dx_2}{d\tau} = x_2 - \dfrac{1}{3}x_2^3 - y_2 + \xi(x_1 - x_2) \\ \dfrac{dy_2}{d\tau} = c(x_2 + a - by_2) \end{cases} \quad (24)$$

where $\tau = \dfrac{t}{\rho C}$, and

$$x_j = \frac{\upsilon_j}{V_0}\ ,\ y_j = \frac{\rho i_{Lj}}{V_0}\ ,\ j = 1,2 \quad (25)$$

$$u_S = \frac{\rho \upsilon_S}{R_S V_0},\ \ \varepsilon = \frac{\rho}{R_S},\ \ \xi = \frac{\rho}{R_C} \quad (26)$$

while ξ is the coupling factor of the system. By choosing a = 0.7, b = 0.8, c = 0.1, $f_N$ = 0.160, ε = 0.150, $U_S$ = 0.0 and $U_0$ = 0.9, the first sub-circuit operates in a chaotic mode (see Fig.5).

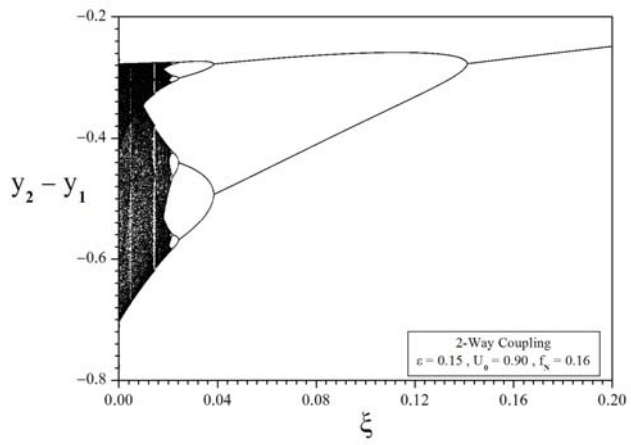


Fig.10. Bifurcation diagram ($y_2 - y_1$) vs. ξ presenting the dynamics of the coupled system of Fig.9.

By increasing the value of coupling factor, the system, starting from a chaotic state, undergoes a reverse period doubling and finally is locked in a period-1 state [7, 8] (see Fig.10).

Considering that the linear coupling resistor plays the role of an electric synapse, we conclude that it can control the chaotic dynamic state of the system.

By coupling one more sub-circuit, we get the system of Fig.11. The bifurcation diagrams vs. the coupling factor are shown in Figs.12-14. The electric synapses control the chaotic behavior, as in the previous case, and lock the system in a periodic state.

## 4 The Coupled System in a Ring Connection

The coupled system in a ring connection is shown in Fig.15. The voltage driven oscillator is 2-way coupled to current driven oscillators forming a ring connection via linear resisting coupling [15,48,49]. All three oscillators have the same circuit parameters.

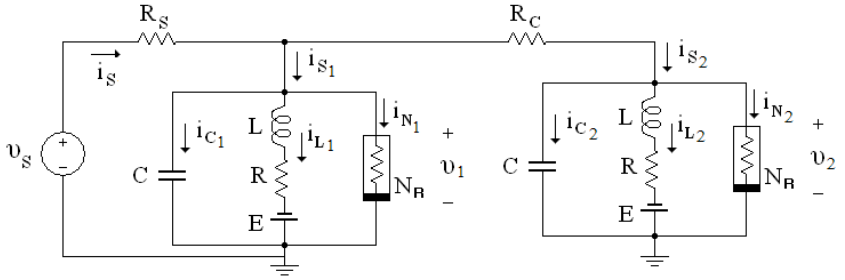


Fig.9. The bidirectional coupled system via the linear resistor.

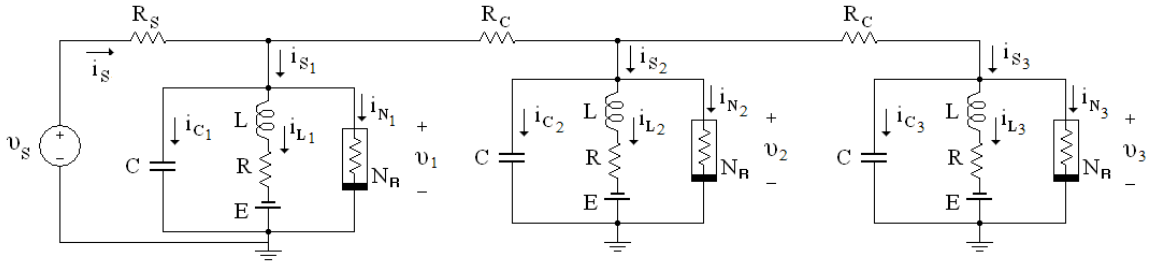


Fig.11. The coupled system consisting of three sub-circuits.

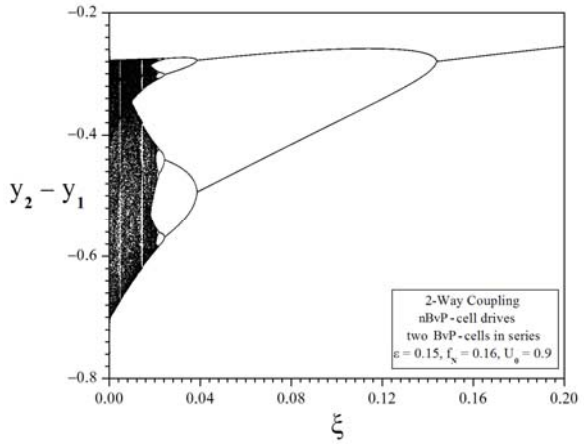


Fig.12. Bifurcation diagram $(y_2 - y_1)$ vs. $\xi$ presenting the dynamics of the coupled system of Fig.11.

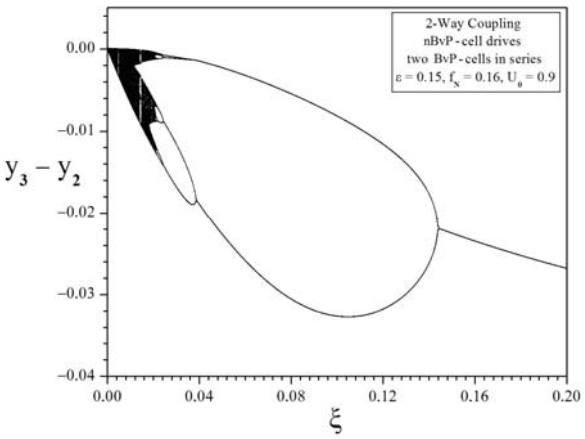


Fig.14. Bifurcation diagram $(y_3 - y_2)$ vs. $\xi$ presenting the dynamics of the coupled system of Fig.11.

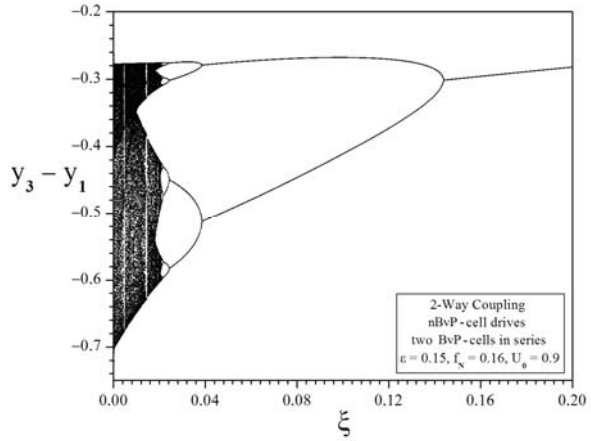


Fig.13. Bifurcation diagram $(y_3 - y_1)$ vs. $\xi$ presenting the dynamics of the coupled system of Fig.11.

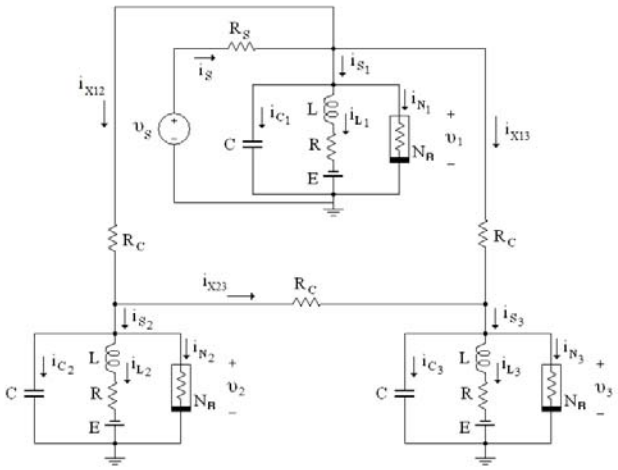


Fig.15. The coupled system in a ring connection.

The υ-i characteristics of the nonlinear resistors are given by the following relationship.

$$i_{Nj} = g(\upsilon_j) = -\frac{1}{\rho}\left(\upsilon_j - \frac{1}{3}\frac{\upsilon_j^3}{V_0^2}\right) \ , \ j = 1,2,3 \qquad (27)$$

Using Kirchhoff's laws the state equations of the system are the following:

$$\begin{cases} \dfrac{d\upsilon_1}{dt} = \dfrac{1}{C}\left\{\dfrac{1}{\rho}\left(\upsilon_1 - \dfrac{1}{3}\dfrac{\upsilon_1^3}{V_0^2}\right) - i_{L1} + \right. \\ \qquad\qquad \left. + \dfrac{\upsilon_S - \upsilon_1}{R_S} - \dfrac{2\upsilon_1 - \upsilon_2 - \upsilon_3}{R_C}\right\} \\ \dfrac{di_{L1}}{dt} = \dfrac{1}{L}\left(\upsilon_1 - Ri_{L1} + E\right) \\ \dfrac{d\upsilon_2}{dt} = \dfrac{1}{C}\left\{\dfrac{1}{\rho}\left(\upsilon_2 - \dfrac{1}{3}\dfrac{\upsilon_2^3}{V_0^2}\right) - i_{L2} + \dfrac{\upsilon_1 - 2\upsilon_2 + \upsilon_3}{R_C}\right\} \\ \dfrac{di_{L2}}{dt} = \dfrac{1}{L}\left(\upsilon_2 - Ri_{L2} + E\right) \\ \dfrac{d\upsilon_3}{dt} = \dfrac{1}{C}\left\{\dfrac{1}{\rho}\left(\upsilon_3 - \dfrac{1}{3}\dfrac{\upsilon_3^3}{V_0^2}\right) - i_{L3} + \dfrac{\upsilon_1 + \upsilon_2 - 2\upsilon_3}{R_C}\right\} \\ \dfrac{di_{L3}}{dt} = \dfrac{1}{L}\left(\upsilon_3 - Ri_{L3} + E\right) \end{cases} \qquad (28)$$

The normalized state equations of the system are:

$$\begin{cases} \dfrac{dx_1}{d\tau} = x_1\left(1-\varepsilon\right) - \dfrac{1}{3}x_1^3 - y_1 - \\ \qquad -\xi\left(2x_1 - x_2 - x_3\right) + u_S \\ \dfrac{dy_1}{d\tau} = c\left(x_1 + a - by_1\right) \\ \dfrac{dx_2}{d\tau} = x_2 - \dfrac{1}{3}x_2^3 - y_2 + \xi\left(x_1 - 2x_2 + x_3\right) \\ \dfrac{dy_2}{d\tau} = c\left(x_2 + a - by_2\right) \\ \dfrac{dx_3}{d\tau} = x_3 - \dfrac{1}{3}x_3^3 - y_3 + \xi\left(x_1 + x_2 - 2x_3\right) \\ \dfrac{dy_3}{d\tau} = c\left(x_3 + a - by_3\right) \end{cases} \qquad (29)$$

where $\tau = \dfrac{t}{\rho C}$ and

$$x_j = \frac{\upsilon_j}{V_0} \ , \ y_j = \frac{\rho i_{Lj}}{V_0} \ , \ j = 1,2,3 \qquad (30)$$

$$u_S = \frac{\rho\upsilon_S}{R_S V_0}, \ \varepsilon = \frac{\rho}{R_S}, \ \xi = \frac{\rho}{R_C} \qquad (31)$$

while ξ is the coupling factor. Keeping the same values of the system parameters, and increasing the value of the coupling factor, the bifurcation diagram of Fig.16 shows the change in dynamics of the voltage driven sub-circuit. The state variables of this sub-circuit, follow a reverse period doubling route from chaos to a period-1 state, while the state variables $x_2$, $y_2$, $x_3$ and $y_3$ have different dynamics. They, very fast, converge to an equilibrium point $Q(x_Q, y_Q)$ for every value of the coupling factor. For ξ = 0,001 we have $Q(x_Q, y_Q)$ = (-1,198, -0,624).

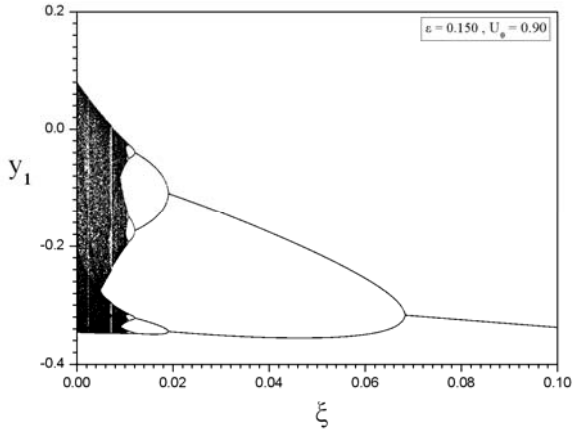


Fig.16. Bifurcation diagram $y_1$ vs. ξ presenting the dynamics of the voltage driven sub-circuit of Fig.15

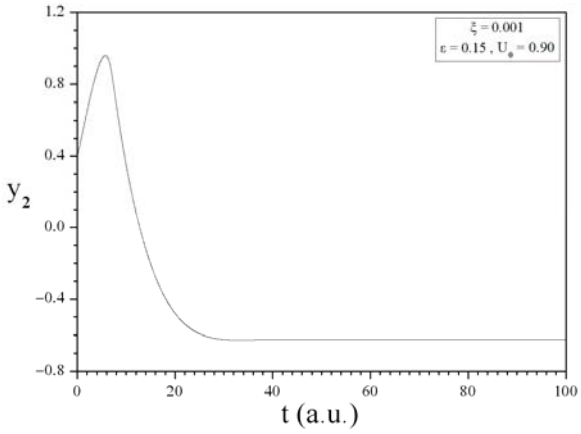


Fig. 17. The waveform of $y_2$ for $\xi = 0.001$.

The waveforms of $y_2$ and $y_3$ as well as their difference $(y_2 - y_3)$ are shown in the figures 17-19, for $\xi = 0.001$, when the voltage driven sub-circuit is in a chaotic state.

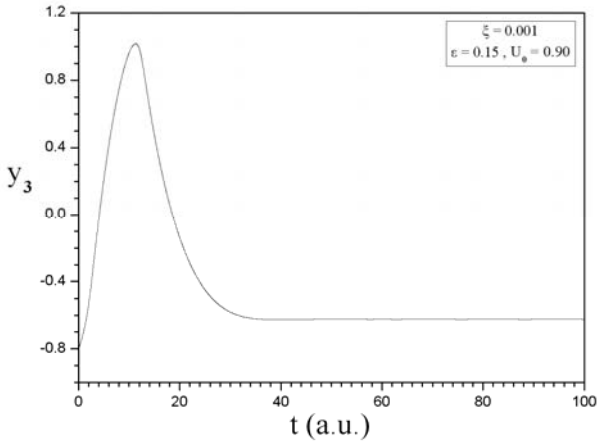


Fig. 18. The waveform of $y_3$ for $\xi = 0.001$.

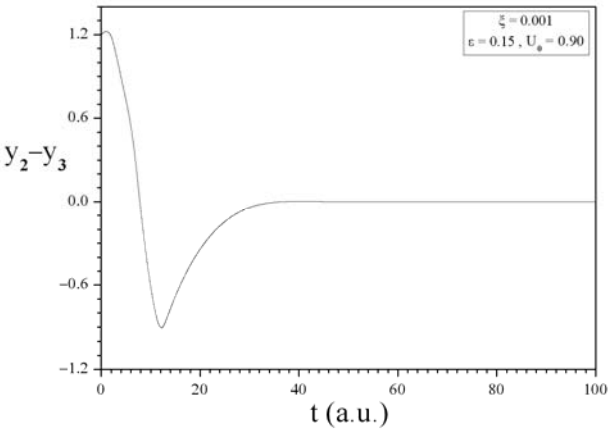


Fig. 19. The waveform of $(y_2 - y_3)$ for $\xi = 0.001$.

## 4.1 Chaotic Synchronization

In order to increase the complexity of the system, we have changed the circuit parameters a, b and c, which are no more identical for all the sub-circuits, while all the other parameters keep the same values. In this case, the state equations of the system (29) take the following form:

$$\begin{cases} \dfrac{dx_1}{d\tau} = x_1(1-\varepsilon) - \dfrac{1}{3}x_1^3 - y_1 - \\ \qquad -\xi(2x_1 - x_2 - x_3) + u_S \\ \dfrac{dy_1}{d\tau} = c_1(x_1 + a_1 - b_1 y_1) \\ \dfrac{dx_2}{d\tau} = x_2 - \dfrac{1}{3}x_2^3 - y_2 + \xi(x_1 - 2x_2 + x_3) \\ \dfrac{dy_2}{d\tau} = c_2(x_2 + a_2 - b_2 y_2) \\ \dfrac{dx_3}{d\tau} = x_3 - \dfrac{1}{3}x_3^3 - y_3 + \xi(x_1 + x_2 - 2x_3) \\ \dfrac{dy_3}{d\tau} = c_3(x_3 + a_3 - b_3 y_3) \end{cases} \quad (32)$$

For the following values of the circuit parameters $a_1 = 0.7$, $b_1 = 0.8$, $c_1 = 0.1$, $a_2 = a_3 = 0.0$, $b_2 = b_3 = 1.0$, $c_2 = c_3 = 0.425$, the bifurcation diagram $(x_2 - x_3)$ vs. $\xi$ is shown in Fig.20. For $\xi > 0.000012$ complete chaotic synchronization between the current driven sub-circuits is observed, while there are not synchronization phenomena between the voltage driven sub-circuit and any current driven sub-circuit (Fig.21). We have to notice, that chaotic synchronization between the current driven sub-circuits is observed because these two circuits are identical. If they are not identical, synchronization is not observed.

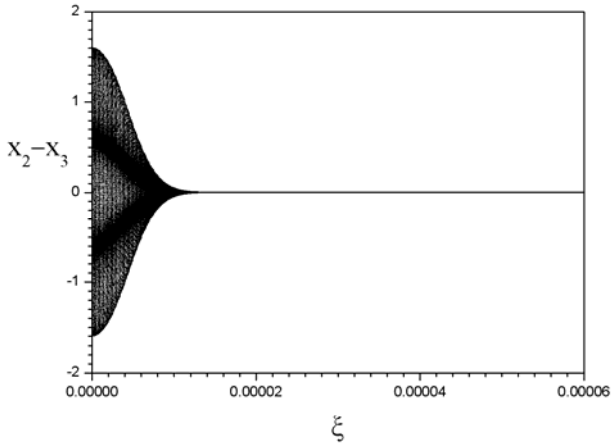


Fig.20. The bifurcation diagram $(x_2 - x_3)$ vs. $\xi$, in the case of different a, b, c parameters of the sub-circuits.

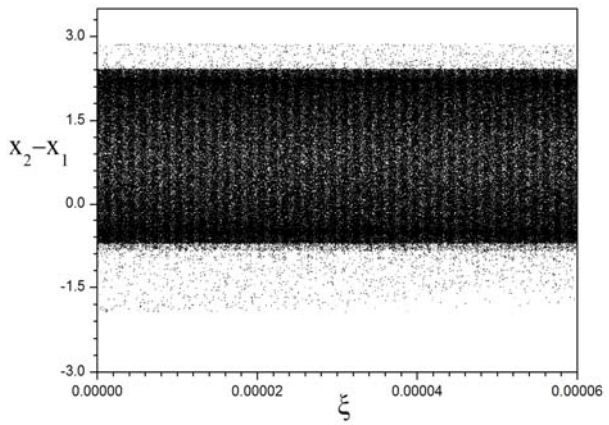


Fig.21. The bifurcation diagram ($x_2 - x_1$) vs. $\xi$, in the case of different a, b, c parameters of the sub-circuits.

## 5 Conclusions

In this paper we have introduced a Bonhoeffer – van der Pol (BvP) electrical oscillator driven by a sinusoidal voltage source and have studied coupled schemes consisting of Bonhoeffer – van der Pol electrical oscillators, which simulate the behavior of coupled neurons. The neurons are coupled via electric synapses, and the linear resistors play this role in the coupled system. In the case of bidirectional coupling, these synapses varying their resistance controlling the dynamics of the neuron cells, from chaotic to periodic states, as it is shown by the bifurcation diagrams. In the case of unidirectional coupling, the dynamics of the coupled system remains chaotic, as the coupling factor is varied. Periodic states are not observed.

In the case of ring-type connection, synchronization is observed in the case that the voltage driven BvP oscillator have different circuit parameters than the two identical current-driven BvP oscillators. The system has very interesting dynamics and its study is in progress.

*References:*

[1] G. Chen and X. Dong, *From Chaos to Order: Perspectives, Methodologies and Applications*, World Scientific, 1998.

[2] A. L. Fradkov and A. Yu. Pogromsky, *Introduction to Control of Oscillations and Chaos*, World Scientific, 1998.

[3] H. Zhang, D. Liu, and Z. Vang, *Controlling Chaos: Suppression, Synchronization and Chaotification*, Springer, 2009

[4] M. A. F. Sanjuan and C. Grebogi, *Recent Progress in Controlling Chaos*, World Scientific, 2010.

[5] S. Boccaletti, C. Grebogi, Y.-C. Lai, H. Mancini, D. Maza, The Control of Chaos: Theory and Applications, *Phys. Reports*, Vol. 329, 2000, pp. 103-197.

[6] E. Ott, C. Grebogi, and J. A. Yorke, Controlling Chaos, *Phys. Rev. Lett*, Vol.64, 1990, pp. 1196-1199.

[7] V. Patidar, N. K. Pareek, and K. K. Sud, Suppression of Chaos Using Mutual Coupling, *Phys. Lett*, Vol.A304, 2002, pp. 121-129.

[8] I. M. Kyprianidis, Ch. Volos, and I. N. Stouboulos, Suppression of Chaos by Linear Resistive Coupling, *WSEAS Trans. Circuits Syst.*, Vol.4, 2005, pp. 527-534.

[9] L. M. Pecora and T. L. Carroll, Synchronization in chaotic systems, *Phys. Rev. Lett.*, Vol. 64, 1990, pp. 821-824.

[10] A. C. J. Luo, A theory for synchronization of dynamical systems, *Commun. Nonlinear Sci. Numer. Simul.*, Vol. 14, 2009, pp. 1901-1951.

[11] A. Pikovsky, M. Rosenblum and J. Kurths, *Synchronization: A universal concept in nonlinear sciences*, Cambridge University Press, 2003.

[12] E. Moselkide, Y. Maistrenko and D. Postnov, *Chaotic synchronization: applications to living systems*, World Scientific, 2002.

[13] S. Boccaletti, J. Kurths, G. Osipov, D. L. Valladares and C. S. Zhou, The synchronization of chaotic systems, *Phys. Rep.*, Vol.366, 2002, pp. 1-101.

[14] I. M. Kyprianidis and I. N. Stouboulos, Synchronization of two resistively coupled nonautonomous and hyperchaotic oscillators, *Chaos Solitons & Fractals*, Vol. 17, 2003, pp. 317-325.

[15] I. M. Kyprianidis and I. N. Stouboulos, Chaotic synchronization of three coupled oscillators with ring connection, *Chaos Solitons & Fractals*, Vol.17, 2003, pp. 327-336.

[16] G. Chen, *Controlling Chaos and Bifurcations in Engineering Systems*, CRC Press, 2000

[17] E. Schöll and H. G. Schuster, (Eds), *Handbook of Chaos Contro*l, Wiley-VCH, 2008.

[18] J. M. Gonzalez-Miranda, *Synchronization and Control of Chaos: An Introduction for Scientists and Engineers*, Imperial College Press, 2004.

[19] B. Lading, E. Moselkide, S. Yanchuk and Y. Maistrenko, Chaotic synchronization between coupled pancreatic β-cells, *Progr. Theor. Phys. Suppl.*, Vol.139, 2000, pp. 164-177.

[20] N.-H. Holstein-Rathiou, K.-P. Yip, O. V. Sosnovtseva and E. Moselkide, Synchronization phenomena in nephron-nephron interaction, *Chaos*, Vol.11, pp. 417-426, 2001.

[21] I.M. Kyprianidis, A. N. Bogiatzi, M. Papadopoulou, I. N. Stouboulos, G. N. Bogiatzis, and T. Bountis, Synchronizing chaotic attractors of Chua's canonical circuit. The case of uncertainty in chaos synchronization, *Int. J. Bifurc. Chaos*, vol. 16, 2006, pp. 1961-1976.

[22] Ch. K. Volos, I. M. Kyprianidis and I. N. Stouboulos, Various synchronization phenomena in bidirectionally coupled double scroll circuits, *Commun Nonlinear Sci Numer Simulat*, Vol.16, 2011, pp. 3356-3366.

[23] Ch. K. Volos, I. M. Kyprianidis and I. N. Stouboulos, Designing a coupling scheme between two chaotic Duffing-type electrical oscillators, *WSEAS Transactions on Circuits and Systems*, Vol.5, 2006, pp. 985-991.

[24] F. Dragan, Controlling Chaos in DC/DC Converters using Ott-Grebogi-Yorke and Pyragas Methods, *WSEAS Trans. Circuits Syst.*, Vol.5, 2006, pp. 849-854.

[25] Y. An, Z. Chen, C. Sun, Z. Liu, K. Yan, K. Warbinek, Control of Chaotic Behavior in Thruster Motor System for Deepwater Ocean Robot, *WSEAS Trans. Circuits Syst.*, Vol.5, 2006, pp. 774-777.

[26] O. Tsakiridis, E. Zervas, E. Lytra, J. Stonham, Two Inputs Electronic Controlled Chaotic Pattern Modulator, *WSEAS Trans. Circuits Syst.*, Vol.4, 2005, pp. 1464-1468.

[27] V. Grigoras, C. Grigoras, Encryption Method Based Non-Additive Discrete-Time Chaos Synchronization, *WSEAS Trans. Circuits Syst.*, Vol.5, 2006, pp. 1608-1613.

[28] I. V. Ermakov, V.Z. Tronciu, P. Colet and C. R. Mirasso, Controlling the unstable emission of a semiconductor laser subject to conventional optical feedback with a filtered feeback branch, *Optics Express*, Vol.17, 2009, pp.8749-8755.

[29] I. Wedekind and U. Parlitz, Synchronization and antisynchronization of chaotic power drop-out and jump-ups of coupled semiconductor lasers, *Phys. Rev. E*, vol.66, 2002, 026218.

[30] S. Sivaprakasam, E. M. Shahverdiev, P. S. Spencer, and K. A. Shore, Experimental demonstration of anticipating synchronization in chaotic semiconductor lasers with optical feedback, *Phys Rev Lett*, vol.87, 2001, 154101.

[31] S. Boccaletti, A. Farini, and F.T. Arecchi, Adaptive synchronization of chaos for secure communication, *Phys Rev E*, Vol.55, 1997, pp. 4979–4981.

[32] A. N. Miliou, I. P. Antoniades, S. G. Stavrinides and A. N. Anagnostopoulos, Secure communication by chaotic synchronization: Robustness under noisy conditions, *Nonlinear Analysis: Real World Applications*, Vol.8, 2007, pp. 1003-1012.

[33] B. Nana, P. Woafo, and S. Domngang, Chaotic synchronization with experimental application to secure communications, *Commun Nonlinear Sci Numer Simulat*, Vol.14, 2009, pp. 2266-2276.

[34] L. Gámez-Guzmán, C. Cruz-Hernández, R. M. López-Gutiérrez, E. E. García-Guerrero, Synchronization of Chua's Circuits with Multiscroll Attractors: Application to Communication, *Commun Nonlinear Sci Numer Simulat*, Vol.14, 2009, pp. 2765-2275.

[35] N. Axmacher, F. Mormann, G. Fernandez, C. E. Elger and J. Fell, Memory formation by neuronal synchronization, *Brain Research Reviews*, Vol.52, 2006, pp. 170-182.

[36] J. Wang, Y. Q. Che, S. S. Zhou and B. Deng, Unidirectional synchronization of Hodgkin-Huxley neurons exposed to ELF electric field, *Chaos Solitons & Fractals*, Vol.39, 2009, pp. 1335-1345.

[37] Q. Y. Wang, Q. S. Lu, G. R. Chen and D. H. Guo, Chaos synchronization of coupled neurons with gap junctions, *Phys. Lett. A*, Vol.356, 2006, pp. 17-25.

[38] M. Aqil, K-S. Hong, M-Y. Jeong, Synchronization of coupled chaotic FitzHugh-Nagumo systems, *Commun Nonlinear Sci Numer Simlat*, Vol.17, 2012, pp. 1615-1627.

[39] R. FitzHugh, Impulses and physiological states in theoretical models of nerve membrane, *Biophys. Journal*, Vol.1, 1961, pp. 445-466.

[40] A. L. Hodgkin and A. F. Huxley, A quantitative description of membrane current and its application to conduction and excitation in nerve, *J. Physiol.*, Vol.117, 1952, pp. 500-544.

[41] J. Nagumo, S. Arimoto, and S. Yoshizawa, An Active Pulse Transmission Line Simulating Nerve Axon, *Proc. IRE*, Vol.50, 1962, pp. 2061-2070.

[42] S. Rajasekar and M. Lakshmanan, Period-Doubling Bifurcations, Chaos, Phase-Locking and Devil's Staircase in a Bonhoeffer – van der Pol oscillator, *Physica D*, Vol.32, 1988, pp. 146-152.

[43] S. Rajasekar and M. Lakshmanan, Algorithms for Controlling Chaotic Motion: Application for the BVP oscillator, *Physica D*, Vol.67, 1993, pp. 282-300.

[44] M. Bier and T. C. Bountis, Remerging Feigenbaum Trees in Dynamical Systems, *Phys. Lett. A*, Vol.104, 1984, pp. 239-244.

[45] I. M. Kyprianidis, P. Haralabidis, I. N. Stouboulos, and T. Bountis, Antimonotonicity and Chaotic Dynamics in a Fourth Order Autonomous Nonlinear Electric Circuit, Int. *J. Bifurcation & Chaos*, Vol.10, 2000, pp. 1903-1915.

[46] I. M. Kyprianidis and M. E. Fotiadou, Complex Dynamics in Chua's Canonical Circuit with a Cubic Nonlinearity, *WSEAS Trans. Circuits Syst.*, Vol.5, 2006, pp. 1036-1043.

[47] I. N. Stouboulos, I. M. Kyprianidis, and M. S. Papadopoulou, Experimental Study of Antimonotonicity in a $4^{th}$ Order Nonlinear Autonomous Electric Circuit, *WSEAS Trans. Circuits Syst.*, Vol.5, 2006, pp. 1662-1668.

[48] Y. Yu, S. Zhang, Global Synchronization of three coupled chaotic systems with ring connection, *Chaos Solitons & Fractals*, Vol.24, 2005, pp. 1233-1242.

[49] Y. Horikawa, Exponential Transient Propagating Oscillations in a Ring of Spiking Neurons with Unidirectional Slow Inhibitory Synaptic Coupling, *J. Theor. Biology*, Vol.289, 2011, pp. 151-159.